Project Description – Project Proposals

Jun.-Prof. Dr.-Ing. Jeanette Hussong; Research Group Laser Measurement Techniques for Multiphase Flows (**LM**); Ruhr-Universität Bochum; phone: +49(0) 234/32-28511; email: jeanette.hussong@rub.de

Jun.-Prof. Dr. rer. nat. Evgeny Guerevich, Chair of Applied Laser Technologies (**LAT**), Ruhr-Universität Bochum; phone: +49(0) 234/32-29891; email: gurevich@lar.rub.de

Wetting of switchable surfaces through magnetically-actuated filaments

---

Project Description

1 State of the art and preliminary work

Lubricant-infused textured solid substrates gain attention as omni-repellent and nonfouling materials [KimAizenberg2013]. Such lubricant-infused surfaces with uniform structures show a shear-tolerant liquid-repellent behavior and low contact angle hysteresis. These favourable properties of liquid infused surfaces shall also be exploited in the present project for actuated liquid infused surfaces. Examples of such surface wetting substrates can be found in nature e.g. for creating airway surface liquid (ASL) transport in the trachea [Chateau2017].
Here, carpets of small hair-shaped filaments, so called cilia, beat in a coordinated fashion to induce a continuous liquid film transport [Hussong2013, Matsui1998]. This principle shall be exploited in the present study by means of biomimetic filament carpets actuated through travelling magnetic fields.
Pre-studies by the petitioners and others have shown that a net fluid transport can be indeed created by such biomimetic filaments through magnetic actuation [Belardi2011, Hussong2011]. However, there remain several challenges. A main challenge is that the magnetic actuation field, the filament motion, and viscous fluid forces of the infused layer and the transported droplet are all interacting, making this a problem of strongly coupled wetting and substrate dynamics.
The strong interaction of magnetic, solid body and fluid and interface forces in combination with large number of actuated filaments, makes the problem extremely computationally expensive. Therefore, recent simulations refer to simplified models, imposing the filament motion [Dauptain2008] or simplifying the viscous fluid interaction as done in the so-called cilia-interaction models [Gueron1993]. This is often done to show that the onset and self-sustaining character of coordinated wavy beating (called metachronal coordination) is the result of hydrodynamic interaction between beating cilia [Gueron1998, Gueron1997, Lenz2006, Guirao2007]. Different continuum models have been developed without resolving the individual filament action usually to simulate mucociliary transport. These are thoroughly reviewed by Smith et al. [Smith2008].
However, due to computational costs, no simulations of the complete, fully resolved problem exist. While most studies using discrete filament models focus on few or individual cilia, Elgeti and Gompper simulated larger array of actuated filaments [Elgeti2013]. Chatelin and Poncet developed a model whose computational cost is only dependent on the number of discretization points and doesn't increase with the number of cilia and performed parametric studies with it [Chatelin2016]. Different models have been chosen to simulate the film transport induced by magnetically moving filament carpets. Gauger et al. [Gauger2006, Gauger2009] and others [Downton2009] simulated a superparamagnetic filament as chain of magnetic and spherical particles that interact by spring forces. This so-called bead-spring model is widely used for filament driven film transport. The influence of the Mason number, that is the ratio between viscous fluid and magnetic dipole forces was studied by Cebers and others numerically [Cebers2003]. Rockenbach et al. performed experiments [Rockenbach2015] and simulations [Rockenbach2016] on a device with rows of flaps on flexible membranes that are actuated by

applying pressure to channels under the membranes. Asymmetry is achieved by the flaps reaching higher into the fluid during the power stroke. Experiment and simulation both show that synchronized beating results in a flow but further breaking the symmetry by tilting the flaps enhances the flow additionally.
Within the last decades, nature inspired, magnetic filaments (often referred to as “artificial cilia” in literature) could be synthesized and externally actuated locally move or mix fluid on sub-millimeter scales. A brief overview of these experimental studies is given by Zhou and Liu [Zhou2008]. From these experimental works, it becomes evident that inducing local fluid motion e.g. for mixing turned out to be much easier to realize than a real transport, that is needed to realize wetting of surfaces. This is partially due to the fact that filaments are often actuated with homogeneous magnetic fields [Fahrni2009, Evans2007]. Hence, to create a net flow individual filaments have to perform a non-reciprocal motion to achieve a net transport in the low Reynold number Stokes regime [Kokot2011, Vilfan2010]. This was partially done by imposing a three-dimensional paddling motion to spm particle seeded rubbery filaments [Vilfan2010, Shields2010]. Maximum net fluid velocities of less than 10 m/s were reported in experimental studies by Shields et al. and Vilfan et al. being too low to create flow rates that can compete with existing microfluidic devices.

Numerically, a wave-like motion between filaments have been proven to enhance fluid transport if combined with an asymmetric beat cycle [Ding2014]. However, to realize a complex, non-reciprocal bending motion of large numbers of micron-sized filaments is very cumbersome explaining why only very few successful studies for transport can be found in literature up to date [Khaderi2013, Shields2010].
Even if a net transport was verified, the flow is dominated by strong oscillations due to synchronized filament motion in a unidirectional magnetic field [Khaderi2013]. In the present project we follow another approach: Pre-studies of the petitioners have shown that a directed actuation force can be created in the Stokes regime through a travelling wave deformation of a thin, porous, liquid-infused layer even with fully reciprocal filament motion. The key mechanism to create a unidirectional net driving force is the modulation of solid phase velocities and porosities along the travelling wave to break the symmetry of the drag force distribution inside the porous layer [Hussong2011b]. The unique kick of the transport mechanism is that it can work for any type of travelling wave motion as long as porosity variations in the porous interlayer are created and it will automatically lead to a uniform, oscillation free liquid transport if a sufficient number of travelling waves are realized. This is of immense importance as it will significantly simplify future technically designed active wetting surfaces based on this actuation principle. Thus, to realize travelling-wave induced droplet transport on liquid-infused surfaces, spatially and temporally rotating magnetic fields have to be created. This challenge will be addressed in WPs1-4.

To verify a uniform wetting effect across the substrate surface, the packing density, elastic, magnetic and geometrical properties of actuated filaments have to be homogenous. Large-area fabrication of microstructures is still a challenging engineering problem when the pattern design should be changed in a flexible way and e.g., fixed masks used in photolithography are not applicable. In this case either self-organization phenomena or mask-less lithography are more useful. In the present project, the 2-Photon Polymerisation (2PP) is chosen as production procedure, being able to create a very homogenous field of filaments (see preliminary works and figures 3 and 4).
The 2-Photon Polymerisation (2PP) was first suggested by Yoh-Han Pao and P. M. Rentzepis in 1965 [Pao1965]. The authors observed polymerisation of styrene monomers induced by radiation of ruby laser at the wavelength $\lambda = 694$ nm although no polymerisation of styrene for radiation of wavelengths $\lambda > 400$ nm had been observed before. The effect can only be explained by simultaneous absorption of two photons, which was first theoretically described in 1931 by Maria Göppert-Mayer [Göppert-Mayer1931].
There are positive and negative photoresists, they differ according to the polymerisation processes happening in the laser-exposed material. In the negative photoresists the exposed structure remains after developing; they are usually used for 2PP. In the positive photoresists the exposed part is removed as the structure is developed. Application of such materials for 2PP is seldom, although these resists allow higher processing velocity especially for microfluidic

structures, in which only a small volume of the polymer in the channel and between the solid structures must be removed.
The two-photon polymerization with negative photoresists was used to develop three-dimensional optical storage memory [Parthenopoulos1989]; now this technique is able to produce arbitrary three-dimensional structures [Kaneko2003] and the resolution of the method may be far beyond the optical diffraction limit. 2PP with structural photopolymers can be applied to a broad range of fields including photonic crystals [Cumpston1999] and micromachines such as microstirrers [Galajda2001], micropumps [Maruno2006] and microtweezers [Maruno2003] and to mimic structural colors in Nature [Zyla2017]. Isolated filaments, the width of which was approximately 20 nm, were achieved by Tan and co-authors [Tan2007], which is the finest 2PP structure reported in the literature to the best of our knowledge. However, if high resolution is not needed, the 2PP technology can be still applied; moreover, in this case the processes can be optimized to increases the production velocity as will be done in the present project to achieve large arrays of actuated filaments within few ours.
Positive photoresists are seldom used for 2PP, because they would be only plausible for structures, in which only a small portion of the polymer is removed, so that the laser beam should expose only a small part of the sample, as it is e.g., in manufacturing of microfluidic devices. Combination of 2PP and positive photoresists is reported only in few papers [Cao2013, Yuan2012, Aumann2014], and it will be also utilized in this project.
To realize actuated filaments, polymers can be mixed with nanoparticles [Guo2014] with remanent properties to be actuated through magnetic fields. Magnetical properties of synthesized filaments strongly depend on the packing density, distribution but also specific nanoparticle properties. To ensure full flexibility of realizing different magnetic properties, not only filaments but also used nanoparticles themselves will be produced by the petitioners. A flexible way of producing nanoparticles is femtosecond laser ablation in liquids [Göcke2017]. Obviously the nanoparticles can be also produced in a chemical way or purchased from commercial providers, however this do not allow rapid and flexible change of the characteristics of the particles and requires the particle purification before mixing them into the polymer. Chemical methods require sometimes application of toxic chemicals and specially equipped chemical labs. Laser ablation allows production of the particles on site or even in one of the components of the photoresist, so that the particles are automatically dispersed there [Guo2014]. This is especially important for magnetic nanoparticles, which quickly agglomerate due to magnetic attractive forces and should be promptly polymerized after production. Superparamagnetic iron nanoparticles can be also generated upon femtosecond iron targets immersed in different liquids [Kanitz2017]. This method was developed in the project DFG GU1075/3 and will be applied in this project.
Studies of the petitioners and co-workers could show, that the amplitude of the motion depends on the interaction between elastic bending forces, viscous fluid forces, magnetic dipole forces and eventually inertial cilia forces [Khaderi2010, Khaderi2013]. If an elongated filament is exposed to an external magnetic field, it will align with the magnetic field vector due to dipole-dipole interactions. If the distribution of particles in the material is homogeneous and the particles are suffciently small, then a filament can be considered as a homogeneous paramagnetic object that experiences a magnetic force and torque. For low actuation frequencies and for non-conducting materials (that is when electric currents can be ignored), the resulting magnetic field can be described by the magnetostatic Maxwell's equations. Due to demagnetization effects inside the filament in the transverse direction, the magnetization vector M is closely aligned with the centerline axis of the cilia. Due to the preferred alignment direction of the magnetization vector with the longitudinal axis of the cilium, the applied magnetic field vector can have a different orientation than the magnetization vector. When the magnetization vector and the magnetic field vector are misaligned, the cilium experiences a magnetic torque. This torque is proportional to the square of the amplitude of the actuation field, and thus it is independent of the sign of the magnetic. Therefore, paramagnetic filaments perform two beat cycles within one full revolution of the magnetic external magnetic field vector [Hussong2011].
The magnetic force acting on a magnetic body of finite size is a gradient force. In an applied homogeneous magnetic field, a gradient force can be induced by the demagnetization field surrounding each filament. Usually, magnetic body forces due to field gradients are neglected in recent studies [Khaderi2009, Alexeev2008, Gauger 2006]. This might change however for

densely packed systems as will be realized in the proposed project. Thus a strong interlink between substrate filaments and actuation field are expected in the present system.
Overall, the bending motion of a filament in a homogeneous magnetic field is driven by the magnetic torque that arises from the phase lag between magnetization vector and magnetic field vector. To fully describe wetting dynamics, the beating motion of a filament has to be described correctly. This is only possible if fluid forces, inertial forces and elastic bending forces of the filament are captured correctly. Thus there exists a strong coupling between wetting and substrate dynamics.
Surely, details of the filament geometry such as form, size and orientation play a great influence. In the present study these aspects are not studied in detail as geometrical optimizations serve for a technical transfer into applications rather than gaining a fundamental understanding of the driving wetting principle proposed here.

Petitioners expertise (LAT)

The activities of the chair of **Applied Laser Technology** are focused on applications of lasers for micro- and nanostructuring and formation of nanoparticles by femtosecond laser ablation in liquids. The two-photon polymerisation (2PP) enables us to produce three-dimensional structures and movable joints with a sub-micrometer spatial resolution, the method is based on polymerisation induced in a photoresist by femtosecond laser pulses with precision much smaller than the wavelength of the laser. The home-made 2PP set up based on the *Tsunami* Ti:sapphire femtosecond laser is shown in Fig. 1. The characteristics of the laser are: wavelength λ=800 nm, pulse duration <100 fs, repetition rate 82 MHz. The laser pulses are focused by the microscope objective (*Carl Zeiss, Plan-Apochromat*, 100x, N.A. =1.4) into a photoresist (i.e., mixture of a monomer and a photoinitiator), in which solid polymer structures are generated upon exposure. The intensity of the laser light controls the degree of polymerization and hence the stiffness of the structure. It can be adjusted by the combination of a wave plate (lambda/2 waveplate) and a polarising beam splitter (BS). The acustooptical modulator (AOM) and the diaphragm are used as a rapid shutter. The xy-galvo scanner and the AOM are controlled by the software developed at the chair, which allows automatic writing of 2PP structures from image or computer-aided design (CAD) files.

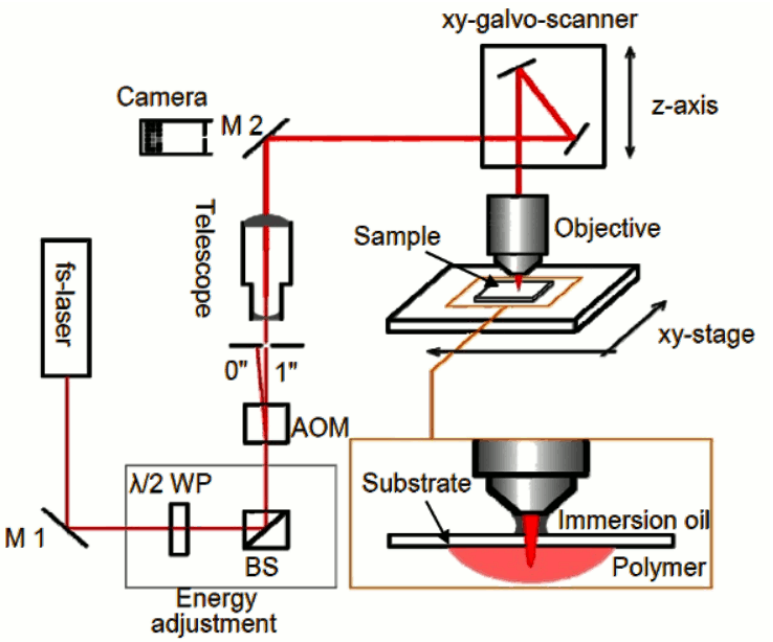

FIGURE 1. Schematic representation of the 2PP setup. BS-beam splitter; M1, M2 – mirrors; lambda/2 WP – wave plate; AOM – acustooptical modulator.

This technique is used in the LAT group to manufacture microstructures with sub-micrometer features, see Fig. 2. The resolution of the technique can be evaluated by *Woodpile structures*, see Fig.2 (a). The width of the lines is approximately 0.4 µm. The resolution of simple structures can be further increased by decreasing the laser exposure, which will, however, result in a decrease in the hardness and in the increasing number of structural defects.

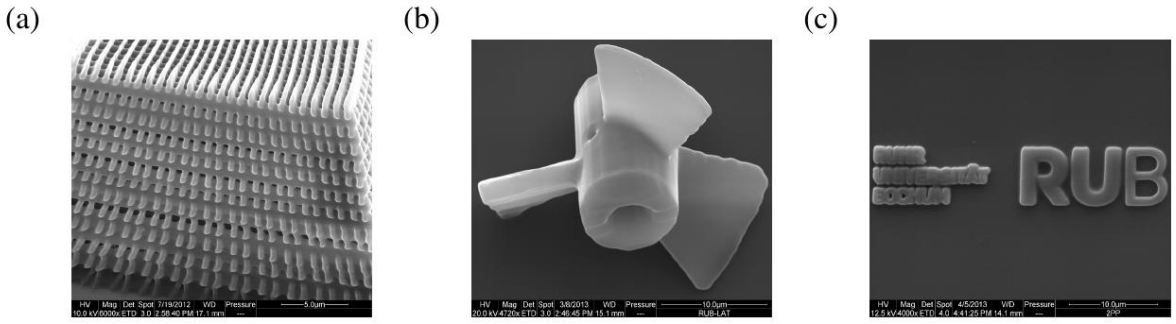

FIGURE 2. Different 2PP structured fabricated with negative photoresists.

For maskless two-photon polymerization negative photoresists are usually applied; however, it can be used also in combination with positive photoresists. One remarkable feature of application of positive photoresists is that the resolution of the microstructures increases with the laser beam scanning velocity, see Fig. 3 (a). Here the laser beam runs several times along the set of parallel and perpendicular lines, which is visible in the SEM image Fig. 3 (b,c,d) by the gaps between the pillars. If laser exposure of the positive photoresist increases, the pillar width becomes modulated along the length, as it can be seen in Fig. 3 (d). Depending on the processing parameters, the 2PP structures may become either rigid or flexible. One can also see from the most right three pillars in the first row in figure 3 (d), that the structures are flexible.

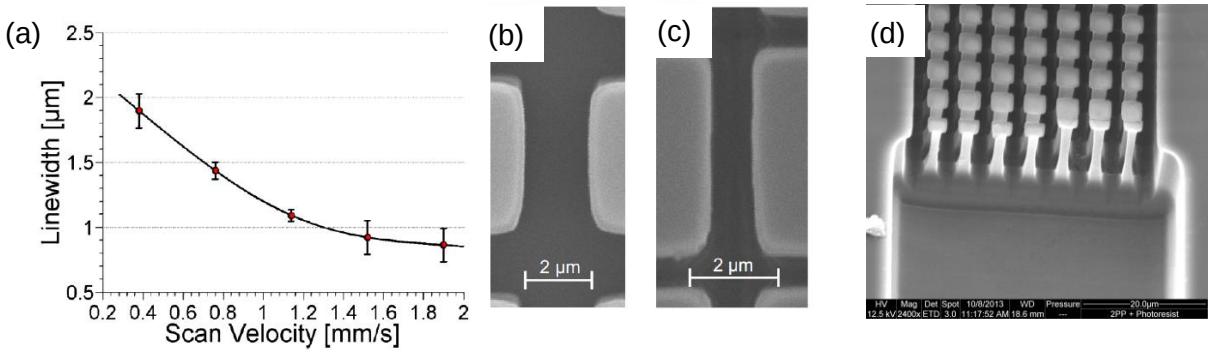

FIGURE 3. 2PP structures fabricated with positive photoresist. (a) the gap between the pillars as a function of the scanning velocity (measured from SEM images, like that shown in subfigures (b) and (c)). (d) side view to the tilted structure. One can see from the most right three pillars in the first row that the structures are flexible [Aumann2014].

Preliminary work (LAT)

Classical two-photon polymerisation requires high-repetition rate, low-pulse energy femtosecond lasers like that used in the experiments described above (82 MHz Tsunami laser). In this case each spot was exposed to approximately one million pulses with an energy of several nanojoules per pulse. Nowadays rapid amplified laser systems with the repetition rate of up to 2 MHz and several tens microjoule pulse energy are available.
At lower repetition rate, the pulses are stronger, so that one single pulse is enough to polymerize a pillar-like structure in the polymer. In this case the shape of the structure is defined by the laser intensity distribution near the focus and cannot be flexibly controlled like it is in traditional 2PP. However, 2 MHz repetition rate lasers allow us to generate up to 2×10^6 hair-shaped filaments per second.

In preliminary experiments with an amplified femtosecond *Tangerine* laser produced by *Amplitude Systems* (wavelength 1030 nm, pulse duration less than 300 fs, setup similar to that shown in figure 1 except of the AOM, which is not required for the single-shot manufacturing) filaments could be successfully created with a single laser shot, see figure 4. For this, the pulse energy was adjusted to meet the compromise between the triggering of the polymerization on the one hand without burning the polymerized material on the other hand. These preliminary experiments demonstrate the feasibility of application of rapid amplified femtosecond lasers for single-shot polymerization. In the present project we aim to realize single-pulse polymerization at 2 MHz. The velocity, at which the surface will be covered with the pillars will then be limited only by the velocity of the galvo-scanner (several meters per second). In this case several square cm will be covered within several seconds.
While in preceding experimental studies the creation of long slender filaments with one free end turned out to be very challenging and time consuming, our polymerization process will be modified to decrease the filament length and increase their stiffness to avoid bending after not-polymerized photoresist is washed away. Modifications of the filament width can be realized by shifting the surface out of the laser surface, varying the energy or increasing the pulse duration by deadjusting compressor inside the femtosecond laser. Details on the procedure are given in WPs 1 and 4.

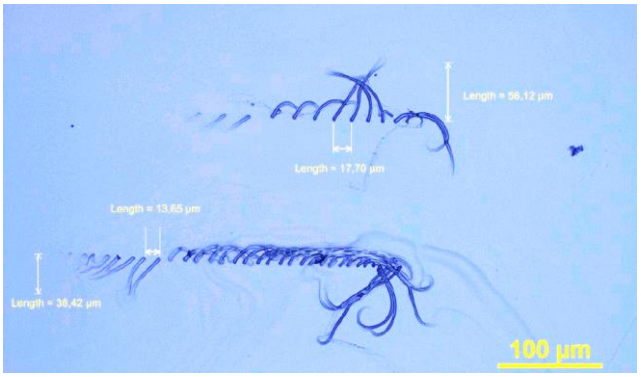

FIGURE 4. Structured generated upon single shot polymerization with an amplified high-repetition rate femtosecond laser. Different groups of flexible polymerized structures (arranged in lines) correspond to different laser parameters.

For successful realization of the project, the polymer structures should be doped with superparamagnetic nanoparticles. Such particles can be either purchased by commercial companies or generated by femtosecond laser ablation of iron targets immersed in different liquids [Kanitz2017]. It was demonstrated that the composition of the liquid influences the ablation rate [Kanitz2017a], chemical composition and the fraction of superparamagnetic particles in the mixture [Kanitz2017].
The main difficulty by embedding nanoparticles into the polymer is their homogeneous distribution in the volume without agglomeration. To increase the homogeneity of the nanoparticle distribution and in order to make the process easier, one of the components of the polymer or the organic solvent can be chosen as the liquid environment for the nanoparticle generation by laser ablation [Guo2014]. Homogeneous distribution of magnetic particles is especially challenging due to attractive forces induced by a small fraction of ferromagnetic particles, which facilitates the particle agglomeration. In the polymer, the agglomerated particles decrease the resolution of the 2PP process because they increase the light scattering [Guo2014]. However, if the required structure is relative simple, then high resolution is not needed, so that we have freedom to optimize the 2PP procedure with respect to the production speed and tolerate some agglomeration, keeping the quality of the structure just as high as needed. In our first experiments we demonstrated that added nanoparticles can be distributed homogeneously enough to create 2PP structures with traditional high-resolution two-photon polymerization [Schröder2018], see Figure 5(a).

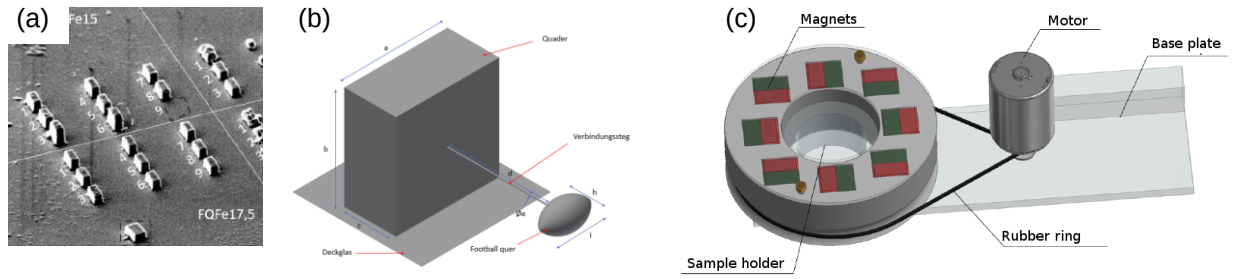

FIGURE 5. (a) 2PP blocks prepared in *Femtobond* photoresist with 5 % of Fe nanoparticles. Quality of the structures depend on the laser processing parameters [Schröder2018]. (b) The STL model of the 2PP magnetic structures shown in the SEM image (a). (c) Model of the setup to generate rotating magnetic field.

Several structures like schematically shown in figure 5 (b) were made in *Femtobond* photoresist with 5 weight % of commercially available Fe nanoparticles. These structures were placed in rotating magnetic field, which was created either by rotating permanent magnets (see figure 5(c)) or by several electromagnets switched on and off with a certain time delay with respect to each other [Köhler2014, Köhler2016].
A set of frames of the structures shown in figure 5 made by CCD camera connected to the optical microscope for different orientations of the external magnetic fields can be seen in figure 6. The orientation of the external magnetic field is indicated by the white arrow. One can see that it is principally possible to make flexible magnetic 2PP structures deflected by external magnetic field. Microstructures actuated by external magnetic field can generate flow in surrounding liquids and can be used as micropumps [Köhler2014, Köhler2016]

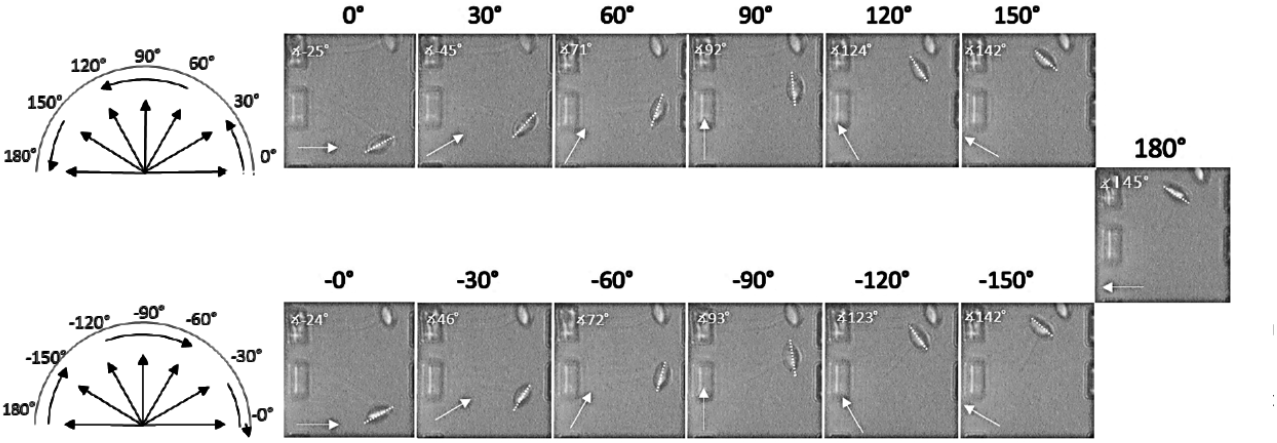

FIGURE 6. Optical microscope images of a flexible magnetic structure (see figure 5 (b)) in external rotating magnetic field. Lower structure is reversibly deflected by the magnetic field.

Petitioners expertise (LM)

In the LM working group, laser measurements are as micro-PIV, Astigmatism-PTV or differential interferometry are combined and adapted to investigate microfluidic and multi-phase flow processes [Kordel2016, Schröer2017]. In addition, combined optical measurement techniques for the investigation of multiphase transient microflows, e.g. cavitation, are being developed in the working group [DFG Project HU2264/1-1]. By combining shadowgraphy and differential interferometry, pressure fields and phase boundaries can be quantified simultaneously to study cavitation and wall interaction as well as the properties of cavitation induced outgassing [Kowalski2018]. One focus is the investigation microparticle dynamics and fractionation in microfluidic systems (Project within the SPP2045, HU2264/3-1). By means of an adapted astigmatism PTV procedure out-of-plane position of 60 Micron particles could be determined in a narrow TC flow with 2 Micrometer accuracy [Schröer2017].

Micro-PIV is used in the research group to determine velocity fields in microfluidic single-phase and multi-phase geometries. Fig. 7(a) shows the experimental setup for micro-PIV and PTV measurements to be used also in the project. An example measurement of a microfluidic flow from a side view determined by micro-PIV with an integrated mirror system behind a 300µm channel stage is shown in Fig.7 (b).

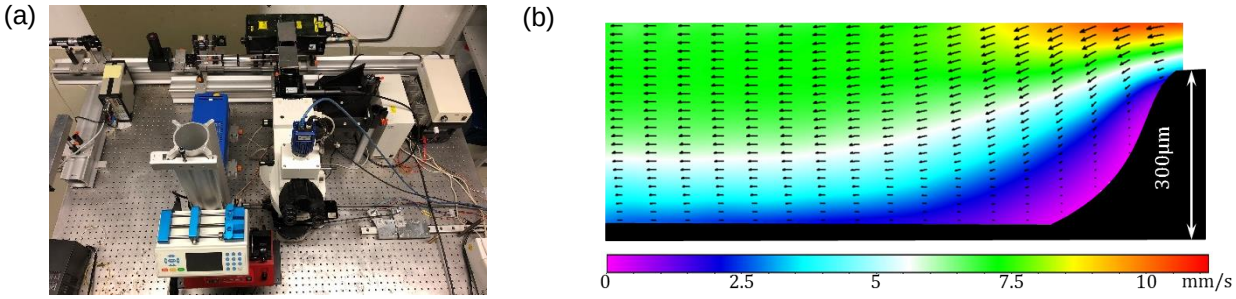

FIGURE 7: (a) Nikon Eclipse epifluorescence microscope for micro-PIV, PTV and Brightfield measurements. Illumination is realized through a double-pulsed ND:YAG laser and recorded with digital cameras (Imager Intense SX, Lavision). (b) Exemplary micro-PIV result of the flow field behind a 300 micrometer channel stage taken with an integrated mirror system in the microchannel to gain a side-view access. The vector field density corresponds to about 17µm, only every fourth vector is shown in flow direction.

Preliminary work (LM)

Numerical studies on wetting induced by travelling wave motions of filament carpets

The research group LM has a long term experience studies on filament driven microflows [7-9]. Combined numerical simulations [6] and micro-PIV/PTV measurements [10] have enabled an improved understanding of basic mechanisms of wall-induced fluid transport in microfluidic actuators.

Numerical studies on the wetting process driven by a wavelike motion of a filament carpet has been investigated, see figure 8 (a). Here, no complex bending motion was considered but a simple in-plane rotation motion of a straight, stiff filament around its base. As such a simple reversible forward-backward motion of a single filament, would not induce any net drag into the fluid. The aim of this numerical study was to prove, that a net film flow can be induced that is purely driven due to the interaction of collectively moving filaments that beat in a time shifted manner inducing travelling waves in the filament carpet. The filament carpet was simulated as porous, actively deforming layer. For this, the Volume Averaged Navier Stokes (VANS) equations were discretized on a staggered and uniform Cartesian grid. An exemplary velocity field is shown in figure 8 (b).

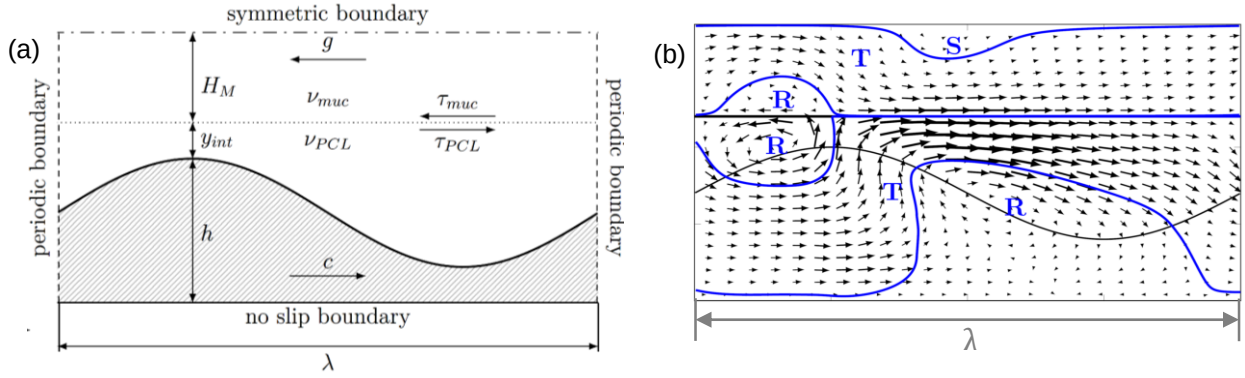

FIGURE 8: (a) VANS simulation of wetting process of a liquid infused, deforming porous layer of height h transporting a viscous fluid layer on top of height H_M against gravity. (b) Velocity field inside the liquid infused porous layer and inside the transported liquid film on top of it. Here, the flow is driven by traction forces at the fluid interface.

The spatial derivatives are estimated with a second-order central-difference scheme. Time integration was done with a second-order Adams-Bashforth scheme and the pressure-gradient term was integrated with the Crank-Nicolson scheme. The VANS equations are solved on an

equidistant Cartesian grid 45000 cells for a wavelength of 3.0. A two-layer liquid system was realized (see figure 8 (b)). Here the liquid infused substrate is driving the wetting process. That is a top liquid film is transported on top of the surface. It could be shown that at low Reynolds numbers, the fluid transport is predominantly driven by the interplay of solid phase velocities and porosity variations as porosity variations break the symmetry of the drag distribution along the filament wave. Infused liquid is transported in the direction of the wavespeed by being continuously ejected from the filament carpet at the wave top and dragged into the filament carpet at the lee side of the wave. The top liquid film is then transported due to viscous shear forces at the liquid-liquid interface. Thus, we show that a travelling wave motion can act as independent transport mechanism. Parameter studies on the Reynoldsnumber, reveal that a maximum transport of fluid is achieved for an intermediate value in the order of one. At higher values a reversing of the fluid flow was observed. In the present project, the influence of the Reynoldsnumber, that is the influence of actuation speed, filament length and fluid viscosity shall be tested.
In the present model direct interaction forces between filaments and top liquid layer or individual droplets can hardly be simulated due to the volume-averaging approach. However, droplets or a liquid film on top of the liquid infused filament carpet may be driven either by direct filament interaction or purely by viscous shear forces at the liquid-liquid interface. The type of interaction between droplet and substrate can be monitored by varying the height of the liquid that is infused in the filament carpet. Both types of driving mechanism shall be investigated experimentally here.

Despite the hydrodynamic proof given by simulations, multiple challenges may be encountered in a real experiment. Therefore, in preliminary works, experiments were performed with a substrate of flap-shaped filaments to proof that micron-sized polymer filament carpets can be indeed actuated in a periodic manner by a rotating magnetic field. Figure 9(a) shows the experimental setup with microfluidic chip (1), fluorescence microscope (2) (LEICA MZ 16 FA FLUO COMBI III), Nd:YAG double pulse laser (3) (New Wave Pegasus PIV-30W), a 12-bit image CCD camera (4) (Imager Intense, LaVision) and the magnetic drive system (5) with the a periodic movement of the micro-actuators is generated.

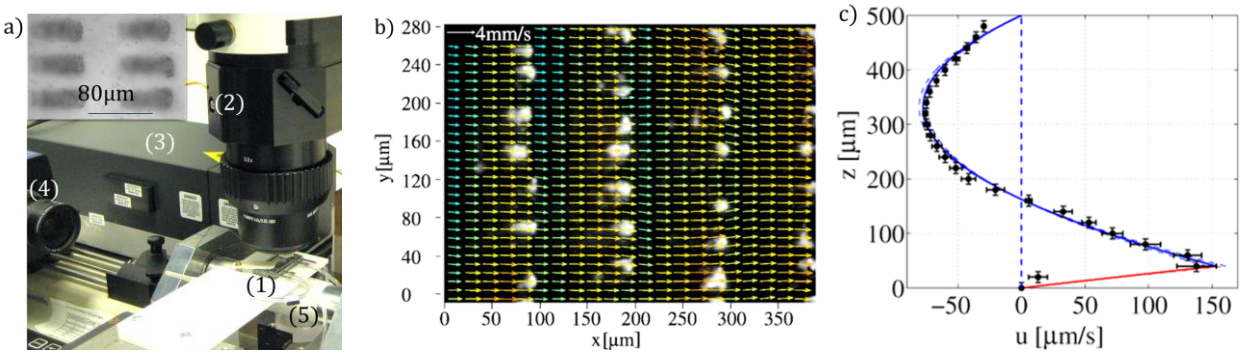

FIGURE 9: a) Micro-PIV set-up with inset of a brightfield image of a micro channel detail with two filament rows. b) Top view of a micro-PIV result of an instantaneous velocity field created by magnetically actuated filaments 60 micron above the substrate surface. c) Phase-averaged velocity profile over the microchannel height taken in a closed fluid chamber of 500 micron height.

A top view of six (out of in total of 10,0000) rectangular microstructures anchored to the channel bottom is shown in the inset of figure 9a). Micro-PIV measurements were taken in the center of the microchannel using Rhodamine-B fluorescent 1.28micron PS particles (Microparticles GmbH). By a synchronous actuator movement, a temporally periodic velocity field is generated in measuring planes parallel to the channel bottom. Phase locked particle images were evaluated based on an ensemble averaging of 100 double frame images. Figure 9 (b) shows an ensemble result of the flow 60 micron above the channel bottom at 10 Hz excitation frequency. A net flow of could be proven by means of phase-locked micro-PIV measurements [7, 8].
Different to the present project, these filaments were created with 2colour lithography, having strong restrictions in packing density due to the production process. Due to low packing densities, a net fluid transport could be only induced if individual filaments would exhibit a non-reciplocal

motion. To realize such a motion is rather complex cyclic motion with a buckling phase of the filament had to be realized. Therefore, in the present project filaments shall be designed to have such low stiffness that they rather align with the magnetic field. They shall move in a similar reversible manner as shown in the simulations. Due to the production procedure proposed here for filament synthesis, an extremely high packing density can be achieved. This is an essential key factor to verify significant porosity variations inside the filament carpet during a travelling-wave actuation and with it a net fluid drag without requiring complex non-reciprocal motion cycles of individual filaments.

Micro-PIV and PTV measurements of liquid transport driven by biological filament surfaces
The wetting principle that will be utilized experimentally in the present project is inspired by nature. Here, wetting and liquid transport of the airway surface is realized in a very efficient manner. To gain insight into the actuation mechanism combined Micro Particle Image Velocimetry (micro-PIV) and Particle Tracking Velocimetry (PTV) on ex vivo tracheal specimens have been performed by the petitioners in cooperation with the Justus-Liebig Universität Giessen [10]. PEG-coated, fluorescent polystyrene particles were used to visualize the flow. While the Particle transport, on the other hand, could be simulated by larger and heavier polystyrene-ferrite particles. Figure 10 (a) shows the reflected light microscope used for the measurements (NIKON ECLIPSE FN1) with sample holder and integrated heating plate (Bioptechs, Butler, PA, USA). Measurements were performed on a prepared tissue sample in a Petri dish. For the measurements a classical micro-PIV setup with dichroic mirror and low pass filter was established as shown in Figure 10 (b). Using a diving lens (Nikon CFIApo40XWNIR) with 40x magnification (NA = 0.8, WD = 3.5 mm), epifluorescence images could be taken over an image area of 222 x 168mm2 at 3 micrometers correlation depth [28, 29]. The measurement volume is exposed with a double-pulsed Nd:YAG laser (SoloPIVIII, NewWave) and particle images are taken with a 12-bit double image CCD camera (ImagerIntense, LaVision). Figure 10 (c) shows a representative result of the combined fluid and particle motion. The fluid flow, which was evaluated by cross correlation and ensemble averaging of 250 images, is represented by the vector field and the velocity amount by a contour plot. The transport of particles influenced by gravity is visualized by particle paths marked in red. Particle transport was evaluated using a simple particle tracking algorithm [10]. In contrast to earlier studies, the investigations have shown that wetting and transport in the respiratory tract is also possible in pure aqueous, and thus Newtonian liquid of low viscosity. Flow velocities of up to 250 mm/s at a distance of 15 microns from the tissue surface could be measured after stimulation.

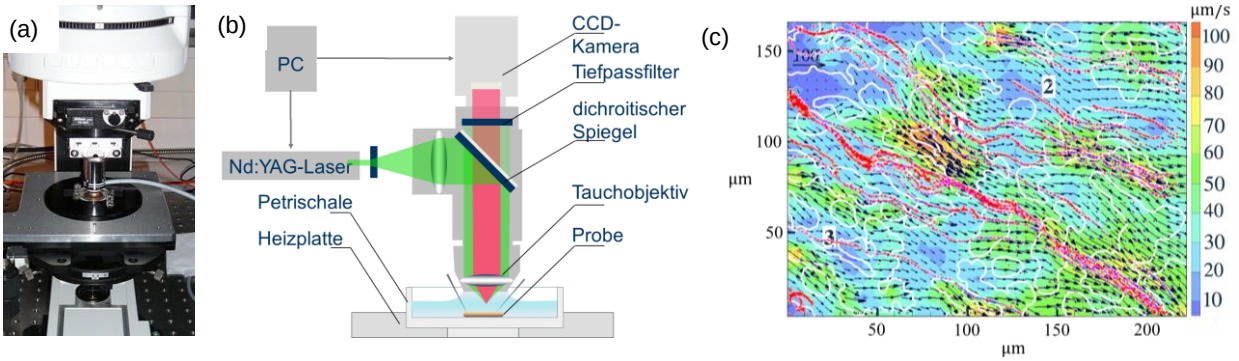

Figure 10: (a) Upright microscope with water dipping lens for Micro-PIV and PTV measurements on film transport induced by biological filament surfaces; (b) Schematic drawing of the micro-PIV set-up; (c) Exemplary result of a combined micro-PIV/PTV measurement on the film flow velocity and the flament driven transport of heavy particles.

In this preliminary studies we demonstrated that different 2PP based techniques are available at the LAT chair (2PP with positive and negative photoresists, and 2PP pillars generated by single laser shots). We also demonstrated that it is principally possible to make magnetic highly-flexible microstructures by two-photon polymerisation.
Furthermore, preliminary numerical studies showed that a travelling wave motion of filaments performing a reciprocal motion leads to a directed net fluid drag that drives the wetting process on a liquid-infused surface. We also showed, that this hydrodynamic transport mechanism works

very efficiently in biological systems, making it very attractive to transfer to technical systems. Finally, preliminary studies showed, that a net fluid transport inside a closed micro chamber may be induced by magnetically actuated filaments of very low packing density if they perform a complex non-reciprocal motion utilizing buckling during the recovery stroke. For the experimental studies, up-to date laser measurement techniques were utilized to characterize both the filament dynamics and the dynamics of the microflow during transport. Throughout the project, we will be able to profit from experiences gained through these extensive numerical and experimental preliminary studies.
In this project we combine up to date laser based production and flow measurement techniques to produce large-areas of magnetically-actuated filaments and to analyze their wetting properties.

1.1 Project-related publications

1.1.1 Articles published by outlets with scientific quality assurance, book publications, and works accepted for publication but not yet published.

1. Gordon Zyla, Alexander Kovalev, Markus Grafen, Evgeny L Gurevich, Cemal Esen, Andreas Ostendorf, and Stanislav Gorb. Generation of bioinspired structural colors via two-photon polymerization. Scientific Reports, 7:17622, 2017.
2. Alexander Kanitz, Jan S. Hoppius, Maria del Mar Sanz, Marco Maicas, Andreas Ostendorf, and Evgeny L. Gurevich. Synthesis of magnetic nanoparticles by ultrashort pulsed laser ablation of iron in different liquids. ChemPhysChem, 18:1155–1164, 2017.
3. J. Köhler, J. Friedrich, A. Ostendorf, and E. L. Gurevich. Characterization of azimuthal and radial velocity fields induced by rotors in flows with a low reynolds number. Phys. Rev. E., 93: 023108, 2016.
4. J. Köhler, R. Ghadiri, S. Ksouri, Q. Guo, E. L. Gurevich, and A. Ostendorf. Generation of microfluidic flow using an optically assembled and magnetically driven microrotor. J. Phys. D: Appl. Phys., 47:505501, 2014.
5. Qingchuan Guo, Reza Ghadiri, Thomas Weigel, Andreas Aumann, Evgeny L. Gurevich, Cemal Esen, Olaf Medenbach, Wei Cheng, Boris Chichkov, and Andreas Ostendorf. Comparison of in situ and ex situ methods for synthesis of two-photon polymerization polymer nanocomposites. Polymers, 6:2037–2050, 2014.
6. Hussong J, Breugem W P, Westerweel J, 2011, A continuum model for flow induced by metachronal coordination between beating cilia. *Journal of Fluid Mechanics*, *684*, 137-162.
7. Hussong J, Schorr N, Belardi J, Prucker O, Rühe J, Westerweel J, 2011, Experimental investigation of the flow induced by artificial cilia. *Lab on a Chip*, *11*(12), 2017-2022.
8. Khaderi, S., Hussong, J., Westerweel, J., den Toonder, J., & Onck, P. (2013). Fluid propulsion using magnetically-actuated artificial cilia–experiments and simulations. *Rsc Advances*, *3*(31), 12735-12742.
9. Khaderi, S. N., Craus, C. B., Hussong, J., Schorr, N., Belardi, J., Westerweel, J., Prucker, O., Rühe, J., den Toonder, J. M. J. & Onck, P. R. (2011). Magnetically-actuated artificial cilia for microfluidic propulsion. *Lab on a Chip*, *11*(12), 2002-2010.
10. Hussong J, Lindken R, Faulhammer P, Noreikat K, Sharp KV, Kummer W, Westerweel J, 2013, Cilia-driven particle and fluid transport over mucus-free mice tracheae. *Journal of biomechanics*, *46*(3), 593-598.

2. Objectives and work programme

2.1 Anticipated total duration of the project

Three years

2.2 Objectives

In the present project we are going to design switchable substrates with flexible superparamagnetic filament arrays exerting a travelling wave motion along the substrate surface to create (1) a switching of surface wetting properties and (2) a unidirectional net driving force in the liquid. The unique kick of both transport mechanism is that it can work for any type of travelling wave motion as long as surface wetting and porosity variations in the filament layer are created.
The proposed project aims to provide the experimental proof of principle, showing that a travelling wave motion of a porous interlayer is sufficient to create a uniform droplet transport in a liquid

infused surface. The aim at the end of three years is to realize a unidirectional droplet transport through a travelling wave of liquid infused filamented substrades.
To correctly capture the coupling between wetting hydrodynamics and substrate properties the interaction between viscous fluid forces, elastic bending forces, magnetic dipole forces as well as secondary effects due to hydrodynamic and magnetic interaction of neighboring filaments have to be considered. To successfully control the process of surface wetting the role of time and length scales on the filament motion but also the global travelling wave properties will be studied closely. The project comprises four main steps: (I) the design and modeling of the substrate, (II) the substrate synthesis and material analysis, (III) the technology and system integration and (IV) the flow characterization and modeling.

1.2 Work programme incl. proposed research methods

WP1: MONTHS: 1-6. Choosing the fabrication method.
Optimal strategy for preparation of surfaces covered by flexible magnetic pillars will be evaluated on the example of a small field covered by 10x10 pillars. Three methods baser on two-photon polymerisation will be tested:

WP1.1: Direct Writing
Direct writing of the pillars with amplified femtosecond laser pulses. In this method the laser pulses are directly focused into transparent polymer and the elongated shape of the laser focus induces photopolymerization and generation of long hair-like structures (see Fig.4). The length of the structures is much larger than expected from the Rayleigh length, which can indicate possible influence of the laser light filamentation in the polymer. This influence will be investigated by stretching the incident femtosecond laser pulses by deadjusting the compressor in the femtoseconfd laser. Most probably the length and the width (hence the mechanical stability of the 2PP pillars) can be changed in a broad range by varying the focusing conditions and the incident pulse energy. Ideally the optimal parameters (pulse width, energy and focusing conditions) will be found for single pulse irradiation to achieve the maximal velocity for the surface coverage. If the structures will remain too flexible and not rigid enough, the stability of the structures can be improved by multiple laser shots.
This is a novel and challenging but the most effective (for our purposes) method, which we successfully tested with clear 'Femtobond' polymer in our preliminary work. First experiments in this WP will be done in pure photopolymer to find roughly the required parameters. Following experiments will be done with magnetic nanocomposites (produced in WP2) because the nanoparticles influence (a) the light scattering in the polymer and (b) mechanical properties of the prepared structure.

WP1.2: 2PP in Positive Photoresists
If after 5 Months the first method should give no results, we will try to make the flexible pillars in positive photopolymer. This type of polymers promises higher writing velocity comparing to commonly-used negative photoresists (see method 3 in WP1) and is suitable for high-precision patterning. However, until now no flexible structures or 2PP with nanocomposites based on such polymers have been reported in the literature. Adding nanoparticles to the polymer shouldn't be problematic. Mechanical flexibility can be achieved by lower pre-bake time or by low-doze exposure of the remaining structure under a UV lamp.

Milestone MS1 after Month 6: Chosen rapid fabrication method of the hair-shaped filaments.
2PP with negative photoresist will be accepted as the main fabrication method if after the 6th month of the project methods (1) and (2) should give no results. This method provide maximal precision, enables flexible structures and is compatible with magnetic nanocomposites. However, the production rate is extremely low so that manufacturing of a 5x5 mm structure will take approximately two days (or one weekend). Our preliminary works demonstrated that this is a promising method and after some optimization of the processing parameters, the quality of the flexible magnetic 2PP structures can approach the quality of rigid structures prepared in pure photopolymers. However due to low production speed we will keep this method for backup if the other methods will be less successful.

WP2: MONTHS: 3-36. Generation of the nanoparticles.
Effective generation method of magnetic nanoparticles by femtosecond laser ablation in liquids was successfully achieved in frames of the DFG project GU1075/3. The only optimization required for this SPP project is the dispersing of the nanoparticles in the polymer. Two strategies will be compared: in-situ (the liquid polymer is used as the environment for the nanoparticle generation); and ex-situ (the nanoparticles will be made in organic solvent and after that dispersed in the polymer). The in-situ method is easier experimentally, since it can be directly combined with the direct laser illumination: iron sample will be used for ablation and the same laser pulse will generate nanoparticles and polymerize the environment. However, the success of this method seems to us rather unlikely. The ex-situ method is compatible with all three methods from the WP1 but will require ultrasonic-tip breaking of nanoparticle agglomerates after mixing with the polymer. The agglomeration in the nanoparticle suspension growth with time, hince only freshly-prepared nanoparticles will be used and this WP will last until the end of the project.

WP3: MONTHS: 5-9. Optimal concentration of nanoparticles.
On the one hand, higher concentration of superparamagnetic nanoparticles will make the structure more responsive to external magnetic field. On the other hand, if the particle concentration will be too high, the scattering of the incident laser light will increase (causing lower resolution of the production method) and the mechanical properties of the pillars will decrease (we assume that they will break more easily under mechanical stress applied). Hence there should be an optimum in the nanoparticle concentration in the structure. If this concentration will be too low to obtain any measurable response on the applied external magnetic field, a new magnetic driver based either on stronger permanent (or electric) magnets will be built except of that used in our previous works [Koehler, Koehler, Kutly].(diese Zitate waren in Prelim.Work und Introduction)

WP4: MONTHS: 6-24. Optimization of the geometry of the structure.
The distance between the pillars is limited by the resolution of the applied method. However, during the developing or operation, the flexible pillars can stick together due to attractive forces induced by liquid bridges between them. Although this effect will reduce reproducibility of the production, it is not necessarily bad, because such agglomerated pillars (if they remain flexible) will just have a smaller flexibility but remain functional. Moreover, this can be used to introduce asymmetry in the system because this agglomeration will disappear as soon as the pillars are completely covered by the liquid.
The liquid transportation can be achieved by asymmetric (irreversible in time) motion of the artificial cilia. This can be achieved in two ways (1) asymmetric shape of the structures; (2) asymmetric excitation. The following strategies will be explored to generate the asymmetric shape of the cilia:
(a) Optical deadjustment of the laser beam with respect to the objective lens will induce beam distortion and inhomogeneous intensity distribution in the laser focus. This will modulate the degree of polymerization and hence, the stiffness of the filament for bending in different lateral directions.
(b) Instead of single shots, a short line in the plane of the substrate will be written by the laser beam. The degree of polymerization at the end of the line will be higher than at the starting point, because the already-polymerized polymer increases the absorption coefficient and thus facilitates the polymerization.
(c) Application of traditional 2PP with positive or negative photoresists. This strategy will be used as the last “backup” option due to low velocity of this manufacturing method.
If asymmetric shape of the filaments will be difficult to realize practically, the asymmetric magnetic field will be applied. To do this, the surface will be surrounded by four or eight electromagnets, and the amplitude of the current in each circuit will be controlled separately.

Milestone MS2 after Month 24: Magnetic filaments for asymmetric kick.
Rapid method for covering surfaces of several square millimeters by flexible magnetic structures for asymmetric kick will be developed. The methods will be validated according to the liquid transport on the surface.

WP5: MONTHS: 1-10. System integration and test measurements
To realize travelling-wave motion of a liquid infused filament carpet for droplet transport, a spatially and temporally rotating magnetic fields has to be created, the measurement set-up has to be established and the filament sample has to be integrated into the set-up to for in-situ temporally and spatially resolved flow measurements.

WP5.1: Design and building of the magnetic actuation system
A spatially and temporally rotating magnetic field will be realized by an array of permanent magnets moved below the substrate, while PIV/PTV measurements on the droplet and liquid transport are performed from a top view with an upright microscope set-up of the LM workgroup. In pre-studies, flap-shaped filaments could be actuated to create a liquid transport with field strengths in the order of 180mT [8]. Similar field strengths shall be realized in the present study using an actuation system comparable to that shown in figure 5(c) used by the LAT workgroup. The basic principle will be to arrange cubic magnets of a few millimeters in alternating orientation to create a magnetic field that changes its magnetic field vector orientation spatially. Placing this array if permanent magnets onto a rotation stage, the rotating magnetic field travels inducing a spatially and temporally periodic filed needed to realize travelling wave motions in the filament array. The challenge will be to achieve a sufficient field strength at a minimum wavelength, that is a minimum spatial distance over which the field vector performs a 180-degree rotation. This is of importance as the driving transport speed is known to scale inversely to the wavelength [6]. Therefore, simulations of the magnetic field in commercial software (e.g. Opera FEA) will be part of the present WP for configuration variations allowing to realize the desired properties of the magnetic field distribution before a magnetic actuation system is built.

WP5.2: Adapting the optical measurement set-up for in-situ measurements
In the research project detailed optical investigations for the characterization of droplet, liquid film motion but also internal circulation and flow pattern formation as well as the filament motion have to be characterized simultaneously. In the LM group, the necessary optical measuring equipment is available for this purpose. Micro-Particle Image Velocimetry (Micro-PIV) or Astigmatism Particle Tracking Velocimetry (A-PTV) will be combined with fluorescence or bright field imaging depending on the specific needs. For this high resolution multicamera measurements will be utilized and synchronized with the actuation system to perform phase-locked measurements with an upright epi-fluorescence microscope (Nicon Eclipse). Fluorescence tracer image series (with pulsed or continuous laser light illumination) are recorded for Micro-PIV or A-PTV. Commercially available spherical, differently fluorescent labeled particles with a particle diameter of 0.6-3 µm (microParticles GmbH) are used. Micro-PIV/A-PTV measurements of the detailed flow field in between the filaments and inside the wetting phase (droplets or liquid film) are essential to gain a better understanding of the wetting principle and to identify emerging circulation areas with growing actuation frequencies. To detect particles, a spatial image resolution of at least 1µm/pixel is required. For this, either a Phantom Miro 110 with a magnification of M=20 and a refresh rate of 1.6 kHz (image range=1280µm x 800µm) or a CCD camera (Imager Intense SX) with 10.8 Hz double frame rate (image range=2058µm x 2456µm at M=3.45) will be used. A scanning method is used to quantify the flow field over the entire liquid film height and cross section of the filament array.

WP5.3: Implementation of substrate into a microfluidic chamber system
To realize droplet or liquid film wetting, an open channel system will be utilized. A channel gasket will be placed on the water-submerged substrate after the polymerisation process is completed. Thus, the sample will remain in a wetted state to avoid damage of the filaments. As the LAT production lab and LM measurement lab of both petitioners are on 3min walking distance, samples will be closed with a simple cover glass and directly placed into the measurement section after production. The open chamber will be designed such that the filament array is located in the middle of the open chamber with space around to the sidewalls. By this a circulating flow can be realized inside the chamber with minimum backpressure over the filamented array. The film height can be easily changed by adding or retreating liquid with a syringe. Due to the small amount of liquid required, only small amounts of fluorescent tracers are required for flow characterization.
As for long measurement champagnes evaporation of the water phase is expected, a syringe pump can provide a continuous release of small amount of water just to compensate this effect.

Pretest will be done to determine the required water supply to ensure a constant water level. Furthermore, the liquid film height will be determined before and after each measurement.
The liquid chamber will be also equipped with a temperature sensor as temperature changes lead to changes in fluid viscosity. Furthermore, an oil droplet releasing capillary will be placed on top of the substrate surface. To generate fresh droplets at regular intervals a second syringe pump will be used. As the working distance of the microscope objectives is typically 10-30mm, there is enough space left to realize these installations. A side viewing mirror holding system will be verified. It will be submerged into the fluid chamber and aligned through a fine traversing system and allows to get a side-view access to different regions of the filament carpet.

WP6: MONTHS: 11-17. Test measurements on liquid infused filament motion
The main purpose of the present WP is to ensure direct feedback loop between filament generation and performance in a liquid state under magnetic actuation. This is essential for the success of the project.

WP6.1: Filament alignment in static fields
Samples produced in the LAT lab will be tested after synthesis in the LM lab. The aim is to find out at an early development stage how well different filament designs can be actuated. In the present WP liquid infused filament carpets will be tested only under quasi static actuation conditions to quantify the maximum motion amplitude that may be performed. For this the optical side-view access through a mirror system as used also for micro-PIV measurements already (see figure 7(b)) will be used. The aim of the WP is to attain information on the orientation and curvature of filaments for different magnetic field vector orientations. The study will be also done for different heights of the infused liquid and also for a two-layer system with an oil film on top to see if filaments may stretch into the oil phase or despite their oil-repellant behavior.

WP6.2: The influence of the actuation speed on the filament motion
The motion of fully submerged filaments will be studied for different actuation speeds of the magnetic field. This study will reveal how the beat cycle of filaments changes due to increasing damping effect induced by viscous fluid forces. Investigations will be done in a fully submerged filament array without wetting phase. The aim is to test a feasible actuation frequency range (in the order of 1-100 Hz), to eventually optimize the magnetic actuation system the filament properties to achieve a maximum deflection response also at higher actuation frequencies. Parts of the characterization will be to quantify the phase lack realized along the filament array as well as the repeatability of the motion. This will be done by means of brightfield imaging from a top and side view into the channel. A significant part of the WP will also be spent on actuation or filament optimization.

WP7: MONTHS: 18-28. Flow measurements and characterization of droplet wetting
The aim of the present WP is a detailed study on the droplet and fluid motion, both inside transported droplets as well as in the liquid layer in which filaments are magnetically actuated.

WP7.1: Droplet creation und preparation
Measurements shall be performed on a droplet-based wetting process. For this oil droplets of different size and viscosity will be created and placed on the liquid infused filament substrate. This is done by using a syringe pump that suspends liquid through a capillary placed closely above the substrate surface. Different droplet viscosities (1x-100x water viscosity) will be tested using silicon oil (Wacker Silicon oil). To characterize the 3D internal droplet circulation during actuation, High-speed A-PTV measurement will be performed. For this, droplets will be doped with fluorescent polystyrene or melanin tracers. Different tracer materials, sizes and seeding densities will be tested to ensure that particles may be fully submerged into the droplet, to ensure a sufficient particle signal strength and density. Different droplet sizes will be realized, using different capillary diameters. Pre-studies will be performed to characterize the droplet size generated with different liquids and capillaries.

WP7.2: measurement of droplet transport and internal 3D droplet circulation
The droplet transport will be measured by phase-locked fluorescence imaging from a top view. For this droplets will be stained with Rhodamine-B. As for a finite number of actuation waves realized within the filament carpet, the net flow is expected to be superposed by an oscillatory

motion, both phase-averaged recordings of the droplet transport and time-resolved measurements on the oscillatory droplet motion can be performed. Furthermore, effects such as deviations in transport direction and droplet deformations can be evaluated.
In the present system, the internal drop circulation will significantly differ from that anticipated in passive systems. As the internal circulation also influences the contact line dynamics, detailed studies on the internal droplet circulation will be performed. Especially, fluctuations due to a cyclic filament beat will be transferred into the droplet, leading to oscillations in the internal flow. Highspeed A-PTV measurement will be performed on fluid tracer seeded droplets. A-PTV is a suitable choice here as systematic evaluation errors known from e.g. Micro-PIV can be avoided on the one hand and 3D particle distributions and 3D particle displacements can be evaluated from time series measurement without the need of time averaging procedures. This is because the effective measurement volume thickness can be adapted to equal the droplet height, such that scanning and time averaging procedures are not required. Pretest are required to test the optical accessibility and to develop a calibration procedure accounting for curved droplet surfaces. For this first calibration tests will be done on stationary droplets. As in WP 6, different filament samples will be tested varying filament stiffness, length and packing density. The internal droplet circulation will be studied for droplets of different sizes and viscosities.

WP7.3: Measurement of fluid transport and filament motion under transported droplets
The presence of a droplet located on top of the liquid-infused substrate will change the beating dynamics of filaments due to a deformation of the liquid film, changed interface conditions due to enhanced shear stresses at the interface and eventually a direct contact with filaments and droplet depending on the infused liquid film height. Therefore, measurements done to characterize the filament motion as done in WP6 have to be repeated here and need to be combined with measurements of the droplet transport. This is done by utilizing a long working distance water dipping lens and mirror system. Utilizing a water dipping lens enables high-quality optical access without disturbances of the open film surface. An integrated 90° mirror provides optical access from a side view. By this, the filament and liquid film motion can be recorded simultaneously. Such a mirror system has been already successfully utilized in pre-studies [Karim2017]. Test measurements have to be performed to ensure that the water-dipping lens is submerged lateral to the streaming direction with a sufficient distance to minimize its effect on the wetting process. Different filament samples will be tested to study the effect of increased filament stiffness, filament length and packing density on the filament and liquid motion during droplet transport. Droplet transport will be studied for droplets of different sizes and viscosities.

WP8: MONTHS: 29-36. Flow measurements and characterization of liquid film wetting
Wetting may be realized by single liquid drops being transported over a surface. However, some applications, complete surface wetting by a continuous liquid film is essential. The characteristics of such a wetting process driven by magnetically actuated filament carpet is the focus in the present WP.

WP8.1: Measurement of film transport and circulation for different filament samples
A two liquid system is generated, with one liquid being infused in the filament carpet to ensure that filaments move in a wetted state. The second liquid film on top shall be transported by the filament carpet to ensure a continuous wetting of the substrate. The dynamics of both liquid films shall be investigated. For this, phase-locked High-speed Micro-PIV are used to measure the phase-averaged and time-resolved flow field during one actuation cycle. These measurements are combined with A-PTV measurements to characterize regions of circulation and out-of plane motion expected at interface close regions (see Fig. 8(b) in preliminary work). The same liquids are chosen as depicted in WP7.1 for droplet generation.

WP8.2: The influence of the film height on the wetting process
Both, the height of the liquid fil infused in the filament carpet as well as the height of liquid film on top, that is to be transported, will have an influence on the filament motion during actuation. This two-way coupling of liquid film heights and actuation is known to be a key aspect for film transport (e.g. in the airway system) and it shall be studied here in detail. Due to the flexible nature of filaments and their high packing density, filaments are expected to only perform an effective beating cycle when being fully submerged. However, they might also stick into the upper liquid

film. In this case they will cross a liquid-liquid interface and encounter different wetting properties. In the present WP parameter studies shall be performed where the height
of both, the wetting film and the infused liquid film will be varied between 0.5-2 times the filament length. Micro-PIV/A-PTV measurements of the induced flow and simultaneous visualization of the filament motion from a top and side view shall be performed.

WP8.3: The role of actuation speed and strength on the wetting dynamics
The wetting process is driven by periodically moving filaments that accelerate the liquid infused in the filament carpet as well as the wetting phase (droplets or a liquid film) through viscous shear forces or direct contact forces. To execute a travelling wave motion as investigated in preliminary work, neighboring filaments have to beat slightly phase shifted. The phase shift magnitude determines the wavelength. The time that a single filament needs to perform a full actuation cycle also corresponds to the time needed by the surface wave to propagate a full wavelength. Thus, the wave speed is determined by the actuation frequency and its role on the filament motion shall be studied here. This is of importance as we anticipate that there is exists an actuation frequency where droplet or liquid film transport maximizes. This is because viscous fluid forces increasingly damp the filament motion with increasing actuation frequency. Thus the amplitude of the filament deflection will decrease with actuation frequency until the system is completely damped out, leading to a zero beating amplitude. When this happens depends on the magnetic field strength. Therefore, different field strengths shall be realized.

WP9: MONTHS: 34-36. Publications and report

2.3 Data handling

The research data gained from the project will be handled according to the guidelines of Ruhr-University Bochum. All scientific results will be published in international peer-reviewed journals and be presented at international conferences. Following our past best practice, parallel to journal submission all manuscripts will be uploaded to the preprint server *arXiv.org* guaranteeing full open access to our results.

2.4 Other information
– not applicable –

2.5 Descriptions of proposed investigations involving experiments on humans, human materials or animals as well as dual use research of concern
– not applicable –

2.6 Information on scientific and financial involvement of international cooperation partners

No close collaboration with researchers based outside Germany is planned. However, research results will be shared on a regular basis with national and international colleagues via seminars, conference contributions, and general academic exchange.

2.7 Information on scientific and financial involvement of international cooperation partners
– not applicable –

2.8 Researchers with whom you have agreed to cooperate on this project

Bastian Rapp and Dorothea Helmer (Karlsruhe Institute of Technology): Superparamagnetic nanoparticles will be generated by femtosecond laser ablation for the project of Bastian Rapp and Dorothea Helmer. They will be used for doping flexible polymer foams in order to control them by external magnetic fields.
Hans Riegler (MPIKG, Postdam): Distribution of the nanoparticles in the polymer (density and homogeneity) can be monitored by measuring the meniscus shape around nanoparticles embedded near the surface. Nanoparticles generated by femtosecond laser ablation can be provided to Hans Riegler.
Stanislav Gorb (Uni Kiel), Cordt Zollfrank (TU München) and Oliver Lieleg (TU München): We will test the applicability of biodegradable cellulose-polymers developed by the group Gorb/Zollfrank/Lieleg for magnetically actuated 2PP structures.

Varlamova/Borcia (BTU Cottbus) and Müller (Jena): Risk management: In the case of laser malfunction it is agreed, that three groups applying for projects with amplified femtosecond systems (Hussong/Gurevich (Bochum); Varlamova/Borcia (Cottbus) and Müller (Jena)) will use facilities of the partners to avoid delays in achieving the project results.
Steffen Hardt (TU Darmstadt) and Arnold Reusken (RWTH Aachen): Joint Astigmatism Particle Tracking Velocimetry (A-PTV) measurements will take place at RUB to characterize the internal 3D drop circulation of surfactant-covered drops on liquid-infused surfaces as studied in the project of Steffen Hardt and Arnold Reusken.
Patrick Huber (TU Hamburg): PIV provided by the RUB team will be used to study the flow in the vicinity of porous surfaces made by the team of Patrick Huber. Laser-generated nanoparticles produced at RUB will be used for the advanced stage of the Project of Patrick Huber.
Gambaryan-Roisman (TU Darmstadt): 2PP magnetic microcolumns used in our project can stick together upon liquid evaporation. These experimental observations will be compared to analytical and numerical calculations, which will be done in the Project of Prof. Gambaryan-Roisman for fiber-covered elastic surfaces.
Svetlana Santer (Uni Potsdam): A periodic actuation may be verified optically or magnetically. We compare dynamics and the maximal reachable transport of drops on such optically (UniPotsdam) and magnetically (RUB) excited surfaces.
Stefan Metzger (FAU, Erlangen): Experimental results on the interaction of wetting liquid and coating (liquid infused layer) will be compared to numerical results of Stefan Metzger.

3. Bibliography

[**Alexeev2008**] Alexeev, A., Yeomans, J. M., & Balazs, A. C. (2008). Designing synthetic, pumping cilia that switch the flow direction in microchannels. Langmuir, 24(21), 12102-12106.
[**Aumann2014**] Aumann, A., Isabelle Ksouri, S., Guo, Q., Sure, C., Gurevich, E. L., & Ostendorf, A. (2014). Resolution and aspect ratio in two-photon lithography of positive photoresist. Journal of Laser Applications, 26(2), 022002.
[**Belardi2011**] Belardi, J., Schorr, N., Prucker, O., & Rühe, J. (2011). Artificial cilia: generation of magnetic actuators in microfluidic systems. Advanced Functional Materials, 21(17), 3314-3320.
[**Cao2013**] Cao, H. Z., Zheng, M. L., Dong, X. Z., Jin, F., Zhao, Z. S., & Duan, X. M. (2013). Two-photon nanolithography of positive photoresist thin film with ultrafast laser direct writing. Applied Physics Letters, 102(20), 201108.
[**Cebers2003**] Cebers, A. (2003). Dynamics of a chain of magnetic particles connected with elastic linkers. Journal of Physics: Condensed Matter, 15(15), S1335.
[**Chateau2017**] Chateau, S., Favier, J., D'ortona, U., & Poncet, S. (2017). Transport efficiency of metachronal waves in 3D cilium arrays immersed in a two-phase flow. Journal of Fluid Mechanics, 824, 931-961.
[**Chatelin2016**] Chatelin, R., & Poncet, P. (2016). A parametric study of mucociliary transport by numerical simulations of 3D non-homogeneous mucus. Journal of biomechanics, 49(9), 1772-1780.
[**Cumpston1999**] Cumpston, B. H., Ananthavel, S. P., Barlow, S., Dyer, D. L., Ehrlich, J. E., Erskine, L. L. & Qin, J. (1999). Two-photon polymerization initiators for three-dimensional optical data storage and microfabrication. Nature, 398(6722), 51.
[**Dauptain2008**] Dauptain, A., Favier, J., & Bottaro, A. (2008). Hydrodynamics of ciliary propulsion. Journal of Fluids and Structures, 24(8), 1156-1165.
[**Ding2014**] Ding, Y., Nawroth, J. C., McFall-Ngai, M. J., & Kanso, E. (2014). Mixing and transport by ciliary carpets: a numerical study. Journal of Fluid Mechanics, 743, 124-140.
[**Downton2009**] Downton, M. T., & Stark, H. (2009). Beating kinematics of magnetically actuated cilia. EPL (Europhysics Letters), 85(4), 44002.
[**Elgeti2013**] Elgeti, J., & Gompper, G. (2013). Emergence of metachronal waves in cilia arrays. Proceedings of the National Academy of Sciences, 201218869.
[**Evans2007**] Evans, B. A., Shields, A. R., Carroll, R. L., Washburn, S., Falvo, M. R., & Superfine, R. (2007). Magnetically actuated nanorod arrays as biomimetic cilia. Nano letters, 7(5), 1428-1434.
[**Fahrni2009**] Fahrni, F., Prins, M. W., & van IJzendoorn, L. J. (2009). Micro-fluidic actuation using magnetic artificial cilia. Lab on a Chip, 9(23), 3413-3421.
[**Galajda2001**] Galajda, P., & Ormos, P. (2001). Complex micromachines produced and driven by light. Applied Physics Letters, 78(2), 249-251.
[**Gauger2006**] Gauger, E., & Stark, H. (2006). Numerical study of a microscopic artificial swimmer. Physical Review E, 74(2), 021907.

[**Gauger2009**] Gauger, E. M., Downton, M. T., & Stark, H. (2009). Fluid transport at low Reynolds number with magnetically actuated artificial cilia. The European Physical Journal E, 28(2), 231-242.
[**Göcke2017**] Gökce, B., Amendola, V., & Barcikowski, S. (2017). Opportunities and challenges for laser synthesis of colloids. ChemPhysChem, 18(9), 983-985.
[**Göppert**-Mayer1931] Göppert-Mayer, M. (1931). Über elementarakte mit zwei quantensprüngen. Annalen der Physik, 401(3), 273-294.
[**Gueron1993**] Gueron, S., & Liron, N. (1993). Simulations of three-dimensional ciliary beats and cilia interactions. Biophysical journal, 65(1), 499.
[**Gueron1997**] Gueron, S., Levit-Gurevich, K., Liron, N., & Blum, J. J. (1997). Cilia internal mechanism and metachronal coordination as the result of hydrodynamical coupling. Proceedings of the National Academy of Sciences, 94(12), 6001-6006.
[**Gueron1998**] Gueron, S., & Levit-Gurevich, K. (1998). Computation of the internal forces in cilia: application to ciliary motion, the effects of viscosity, and cilia interactions. Biophysical Journal, 74(4), 1658-1676.
[**Guirao2007**] Guirao, B., & Joanny, J. F. (2007). Spontaneous creation of macroscopic flow and metachronal waves in an array of cilia. Biophysical journal, 92(6), 1900-1917.
[**Guo2014**] Guo, Q., Ghadiri, R., Weigel, T., Aumann, A., Gurevich, E. L., Esen, C & Ostendorf, A. (2014). Comparison of in situ and ex situ methods for synthesis of two-photon polymerization polymer nanocomposites. Polymers, 6(7), 2037-2050.
[**Hussong2011**] Hussong, J., Schorr, N., Belardi, J., Prucker, O., Rühe, J., & Westerweel, J. (2011). Experimental investigation of the flow induced by artificial cilia. Lab on a Chip, 11(12), 2017-2022.
[**Hussong2011b**] Hussong, J., Breugem, W. P., & Westerweel, J. (2011). A continuum model for flow induced by metachronal coordination between beating cilia. Journal of fluid mechanics, 684, 137-162.
[**Hussong2013**] Hussong J, Lindken R, Faulhammer P, Noreikat K, Sharp KV, Kummer W, Westerweel J, 2013, Cilia-driven particle and fluid transport over mucus-free mice tracheae. Journal of biomechanics, 46(3), 593-598
[**Kaneko2003**] Kaneko, K., Sun, H. B., Duan, X. M., & Kawata, S. (2003). Submicron diamond-lattice photonic crystals produced by two-photon laser nanofabrication. Applied physics letters, 83(11), 2091-2093.
[**Kanitz2017**] Kanitz, A., Hoppius, J. S., del Mar Sanz, M., Maicas, M., Ostendorf, A., & Gurevich, E. L. (2017). Synthesis of magnetic nanoparticles by ultrashort pulsed laser ablation of iron in different liquids. ChemPhysChem, 18(9), 1155-1164.
[**Kanitz2017a**] Kanitz, A., Hoppius, J. S., Fiebrandt, M., Awakowicz, P., Esen, C., Ostendorf, A., & Gurevich, E. L. (2017). Impact of liquid environment on femtosecond laser ablation. Applied Physics A, 123(11), 674.
[**Karim2017**] Karim, E. (2017). Surface wettability of stainless-steel by laser ablation under different liquid environments. Master Thesis, Ruhr-Universiät Bochum.
[**Khaderi2009**] Khaderi, S. N., Baltussen, M. G. H. M., Anderson, P. D., Ioan, D., Den Toonder, J. M. J., & Onck, P. R. (2009). Nature-inspired microfluidic propulsion using magnetic actuation. Physical Review E, 79(4), 046304.
[**Khaderi2010**] Khaderi, S. N., Baltussen, M. G. H. M., Anderson, P. D., Den Toonder, J. M. J., & Onck, P. R. (2010). Breaking of symmetry in microfluidic propulsion driven by artificial cilia. Physical Review E, 82(2), 027302.
[**Khaderi2013**] Khaderi, S., Hussong, J., Westerweel, J., den Toonder, J., & Onck, P. (2013). Fluid propulsion using magnetically-actuated artificial cilia–experiments and simulations. Rsc Advances, 3(31), 12735-12742.
[**Köhler2014**] Köhler, J., Ghadiri, R., Ksouri, S. I., Guo, Q., Gurevich, E. L., & Ostendorf, A. (2014). Generation of microfluidic flow using an optically assembled and magnetically driven microrotor. Journal of Physics D: Applied Physics, 47(50), 505501.
[**Köhler2016**] Köhler, J., Friedrich, J., Ostendorf, A., & Gurevich, E. L. (2016). Characterization of azimuthal and radial velocity fields induced by rotors in flows with a low Reynolds number. Physical Review E, 93(2), 023108.
[**Kokot2011**] Kokot, G., Vilfan, M., Osterman, N., Vilfan, A., Kavčič, B., Poberaj, I., & Babič, D. (2011). Measurement of fluid flow generated by artificial cilia. Biomicrofluidics, 5(3), 034103.
[**Kordel2016**] Kordel, S., Nowak, T., Skoda, R., & Hussong, J. (2016). Combined density gradient and velocity field measurements in transient flows by means of Differential Interferometry and Long-range µPIV. Experiments in Fluids, 57(9), 138.
[**Kowalski2018**] Kowalski, K., Pollak, S., Skoda, R., & Hussong, J. (2018). Experimental Study on Cavitation-Induced Air Release in Orifice Flows. Journal of Fluids Engineering, 140(6), 061201.
[**Lenz2006**] Lenz, P., & Ryskin, A. (2006). Collective effects in ciliar arrays. Physical biology, 3(4), 285.
[**Maruno2003**] Maruo, S., Ikuta, K., & Korogi, H. (2003). Submicron manipulation tools driven by light in a liquid. Applied Physics Letters, 82(1), 133-135.
[**Maruno2006**] Maruo, S., & Inoue, H. (2006). Optically driven micropump produced by three-dimensional two-photon microfabrication. Applied Physics Letters, 89(14), 144101.

[**Matsui1998**] Matsui, H., Randell, S. H., Peretti, S. W., Davis, C. W., & Boucher, R. C. (1998). Coordinated clearance of periciliary liquid and mucus from airway surfaces. The Journal of clinical investigation, 102(6), 1125-1131.
[**Pao1965**] Pao, Y. H., & Rentzepis, P. M. (1965). Laser-Induced Production of Free Radicals in Organic Compounds. Applied Physics Letters, 6(5), 93-95.
[**Parthenopoulos1989**] Parthenopoulos, D. A., & Rentzepis, P. M. (1989). Three-dimensional optical storage memory. Science, 245(4920), 843-845.
[**Rockenbach2015**] Rockenbach, A., Mikulich, V., Brücker, C., & Schnakenberg, U. (2015). Fluid transport via pneumatically actuated waves on a ciliated wall. Journal of Micromechanics and Microengineering, 25(12), 125009.
[**Rockenbach2016**] Rockenbach, A., & Schnakenberg, U. (2016). The influence of flap inclination angle on fluid transport at ciliated walls. Journal of Micromechanics and Microengineering, 27(1), 015007.
[**Schröder2018**] Schröder, l. C. (2018). Herstellung von magnetischen Mikroaktoren durch Zwei-Photonen-Polymerisation. Master Thesis, Ruhr-Universiät Bochum.
[**Schröer2017**] Schröer, K., Kurzeja, P., Schulz, S., Brockmann, P., Hussong, J., Janas, P. & Wolf, D. E. (2017). Dilute suspensions in annular shear flow under gravity: simulation and experiment. In EPJ Web of Conferences (Vol. 140, p. 09034). EDP Sciences.
[**Shields2010**] Shields, A. R., Fiser, B. L., Evans, B. A., Falvo, M. R., Washburn, S., & Superfine, R. (2010). Biomimetic cilia arrays generate simultaneous pumping and mixing regimes. Proceedings of the National Academy of Sciences.
[**Smith2008**] Smith, D. J., Gaffney, E. A., & Blake, J. R. (2008). Modelling mucociliary clearance. Respiratory physiology & neurobiology, 163(1-3), 178-188.
[**Tan2007**] Tan, D., Li, Y., Qi, F., Yang, H., Gong, Q., Dong, X., & Duan, X. (2007). Reduction in feature size of two-photon polymerization using SCR500. Applied physics letters, 90(7), 071106.
[**Vilfan2010**] Vilfan, M., Potočnik, A., Kavčič, B., Osterman, N., Poberaj, I., Vilfan, A., & Babič, D. (2010). Self-assembled artificial cilia. Proceedings of the National Academy of Sciences, 107(5), 1844-1847.
[**Yuan2012**] Yuan, H., Zhao, Y., & Wu, F. (2012). Two-photon acid generation systems based on dibenzylidene ketone dyes intermolecular sensitization. Chemistry of Materials, 24(7), 1371-1377.
[**Zhou2008**] Zhou, Z. G., & Liu, Z. W. (2008). Biomimetic cilia based on MEMS technology. Journal of Bionic Engineering, 5(4), 358-365.
[**Zyla2017**] Zyla, G., Kovalev, A., Grafen, M., Gurevich, E. L., Esen, C., Ostendorf, A., & Gorb, S. (2017). Generation of bioinspired structural colors via two-photon polymerization. Scientific reports, 7(1), 17622.

4. Requested modules/funds

4.1 Basic Module

4.1.1 Funding for Staff

LM
One Doctoral Student (requested by J. Hussong), who will process the experimental WPs 5-9 of the project. (TVL-13, 36 Months, effectively 75%).
The PhD student will perform all flow measurements (WPs 5-9) at research group LM planned in this project. The student needs to have a strong background in fluid dynamics and microflows as well as experience in handling laser measurement techniques.

LAT
One Doctoral Student (requested by E. Gurevich), who will process the experimental WPs 1-4 and 9 of the project. (TVL-13, 36 Months, effectively 75%).

The PhD student will be responsible for the processing WPs 1-4. The student will also be responsible for documentation of the experiments, communication with the LM department and publication of the results in journals and on international conferences.

4.1.2 Direct Project Costs

4.1.2.1 Equipment up to Euro 10,000, Software and Consumables

LM

-	Electronics and mechanical components for permanent	1500,- €
	magnet actuation system	3000,- €

- Consumables (magnets, fluorescent PEG-coated microparticles, flow connectors, tubing, adaptors, liquids etc.) 1200,- €
- High NA 40X Nikon CFI Plan Fluor-Objective

LAT

- Photopolymers, chemicals, iron targets for making 2PP structure and iron targets for superparamagnetic particles 6000,- €

Total (LM+LAT) for 3 years: **11700,- €**

4.1.2.2 Travel Expenses

LM

- 21th Int. Conference on Experimental Fluid Mechanics (ICEFM 2019), 2019 2000,- €
- European Fluid Mechanics Conference (EFMC 13), 2020 2000,- €
- GALA Fachtagung 2021, „Lasermethoden in der Strömungsmesstechnik“ 1000,- €

LAT

- E-MRS 2019 1500,- €
- E-MRS 2020 1500,- €
- E-MRS 2021 1500,- €

E-MRS conference is one of the most important conferences on laser micro- and nano-processing and development of new materials and their applications.

Total (LM+LAT) for 3 years: **9500,- €**

4.1.2.3 Visiting Researchers – not applicable –

4.1.2.4 Expenses for Laboratory Animals – not applicable –

4.1.2.5 Other Costs – not applicable –

4.1.2.6 Project-related publication expenses

LM 750 Euro p.a.= 2250,- €
LAT 750 Euro p.a.= 2250,- €

4.1.3 Instrumentation – not applicable –

5. Project requirements

5.1 Employment status information

Jun.-Prof. Dr. Evgeny Gurevich: Juniorprofessor, fixed-term contract till 31.12.2018. Confirmation that the position will be extended at least until end of May 2021 is included.

Jun.-Prof. Dr.-Ing. Jeanette Hussong: Juniorprofessor, fixed-term contract till 31.08.2019. Confirmation that the position will be extended at least until end of December 2021 is included.

5.2 First-time proposal data – not applicable –

5.3 Composition of the project group

Jun.-Prof. Dr.-Ing. Jeanette Hussong, LM: Responsible for the supervision of WPs 5-9 (paid by the university).
Jun.-Prof. Dr. Evgeny Gurevich, LAT: is responsible for the 2PP part of the project (paid by the university)
Dipl.-Ing. R. Nett, LAT Technician, organizes working conditions, technical support and the laser safety (paid by the university).
Tukalov, Artem, LM Technician, mechanical workshop, budget funds (paid by the university).

5.4 Cooperation with other researchers

5.4.1 Researchers with whom you have agreed to cooperate on this project

- please see section 2.8 -

5.4.2 Researchers with whom you have collaborated scientifically within the past three years

E. Gurevich:
N. Bulgakova, HiLASE, Prague (Czech Republic);
L. Orazi, Universita degli Studi di Modena e Reggio Emilia (Italy);
Han Gardeniers, Univ. Twente, Enschede (Netherlands);
S. Mathur, Univ. Köln (Germany);
S. Gorb, Univ. Kiel (Germany);
A. Ostendorf, Ruhr-Univ. Bochum (Germany);
G. Laplanche, Ruhr-Univ. Bochum (Germany)
U. Thiele, S. Gurevich, University of Münster (Germany)
C. Zollfrank, TU München (Germany)

J. Hussong:
Luca Brandt, KTH Stockholm (Sweden)
Raffaella Ocone, Heriot-Watt University, Edinburgh (UK)
Andreas Kempf, Universität Duisburg-Essen (Germany)
Dietrich Wolf, Universität Duisburg-Essen (Germany)
Harald Kruggel-Emden, TU Berlin (Germany)
Arno Kwade, TU-Braunschweig (Germany)
Wolfgang Tillmann, TU Dortmund (Germany)
Romuald Skoda, Ruhr-Universität Bochum (Germany)

5.5 Scientific equipment

LM

1. Nicon Eclipse Epifluorescence Microscope
2. Phantom Miro 110 Highspeed camera (1280 x 800 pixel; 1630 fps)
3. Highspeed LED (IL-105b LED Illuminator, pulse width 200ns)
4. 2xDouble-pulsed Nd:YAG-Laser (70mJ Evergreen, Quantel)
5. 2x12-bit dual-frame CCD-cameras (Imager ProSX 5M, Lavision)
6. Computer, recording and evaluation Software for PIV (Lavision)
7. 2xsyringe pumps (Landgraf Laborsysteme HLL GmbH, Typ LA-800)
8. In-house calibration and evaluation software for A-PTV measurements

LAT

1. Home-built 2PP system based on Tsunami femtosecond laser.
2. Tangerine amplified laser system (1030 nm, 20 W, pulse duration 280 fs, 2 MHz)
3. Spitfire amplified laser system (800 nm, 4 W, pulse duration 35 fs, 5 kHz)
4. JenLas D2fs amplified laser system (1025 nm, 4 W, pulse duration 400 fs, 200 kHz)
5. SEM (Scanning Electron Microscope) Zeiss, EVO MA10
6. White-light interferometer Polytec, TMS 1200
7. DLS device for nanoparticle characterisation Microtrac, Nanotrac Wave
8. Optical microscope Nicon, Eclipse LV100
9. Raman Microscope Renishaw
10. Homebuilt contact angle measurement set-up